Research Article

Multidetector Computed Tomography Imaging Features of Inflammatory Myofibroblastic Tumors of the Gastrointestinal Tract in Adults: Radiological, Histopathological, and Immunohistochemical Features

In Young Choi [1], Suk Keu Yeom [1, *], Beom Jin Park [2], Deuk Jae Sung [2], Min Ju Kim [2], Na Yeon Han [2], Yang Shin Park [3], Sang Hoon Cha [1], So Yeon Kim [4] and Jung-Woo Choi [5]

[1]Department of Radiology, Korea University Ansan Hospital, Ansan-si, Korea
[2]Department of Radiology, Korea University Anam Hospital, Seoul, Korea
[3]Department of Radiology, Korea University Guro Hospital, Seoul, Korea
[4]Department of Radiology and Research Institute of Radiology, Asan Medical Center, University of Ulsan College of Medicine, Seoul, Korea
[5]Department of Pathology, Korea University Ansan Hospital, Ansan-si, Korea

*Corresponding author: Associate Professor, Department of Radiology, Korea University Ansan Hospital, 123 Jeokgeum-ro, Danwon-gu, P. O. Box: 15355, Ansan, Korea. Email: pagoda20@gmail.com

Abstract

Background: Inflammatory myofibroblastic tumors (IMTs) of the gastrointestinal (GI) tract are rare phenomena, and the computed tomography (CT) findings of GI IMTs are not well-established.

Objectives: To describe the characteristics of CT scans, pathological specimens, and histological subtypes of GI IMTs in adults.

Patients and Methods: The multidetector computed tomography (MDCT) scans of 11 adult patients (8 males, 3 females; age range, 19 - 76 years) with pathologically proven GI tract IMTs (stomach, small bowel, and colon) were retrospectively evaluated by two abdominal radiologists. The radiological features of IMTs were investigated. The imaging features were correlated with three microscopic IMT subtypes (myxoid vascular, spindle cell, and hypocellular fibrous). Immunohistochemistry was also performed on the specimens, including smooth muscle actin (SMA), vimentin, desmin, S-100, and anaplastic lymphoma kinase.

Results: The tumor size ranged from 1.4 to 15 cm (mean, 5.7 cm). Two growth patterns were classified, namely, wall-thickening (n = 3) and solitary mass-forming (n = 8) patterns; each pattern was matched with a characteristic pathological subtype. All solitary, well-circumscribed masses corresponded to the spindle cell type. Low-attenuation wall thickening with perienteric infiltration was observed in three patients with a wall-thickening pattern. All solitary, well-circumscribed masses (n = 8) showed homogeneous enhancement with variable internal low attenuation, correlated with cystic degeneration, necrosis, myxoid change (n = 6), and hemorrhagic necrosis (n = 2). No patient showed bowel obstruction, while one patient showed regional lymphadenopathy. Immunophenotypes were not correlated with any growth pattern or histological subtype.

Conclusion: The GI IMTs can be classified into two patterns, including wall-thickening and well-circumscribed masses, each matched with a characteristic pathological subtype, which can help explain the tumor behavior. Concomitant CT findings may also provide diagnostic clues for IMT.

Keywords: Stomach, Intestines, Multidetector Computed Tomography, Neoplasms, Granuloma

1. Background

In 1954, inflammatory pseudotumors were first described by Umiker and Iverson to represent a wide spectrum of reactive and neoplastic lesions with common histological features, namely, cytological benign spindle cell proliferation and chronic inflammatory cell infiltration (1-3). Since then, these pseudotumors have been synonymously referred to as plasma cell granuloma, inflammatory myofibroblastic tumor, inflammatory myofibrohistiocytic proliferation, xanthomatous pseudotumor, fibrous xanthoma, xanthogranuloma, plasma cell/histiocytoma complex, plasmacytoma, inflammatory fibrosarcoma, and solitary mast cell granuloma (4-6); these terms are synonymous and in common use. They all exhibit identical pathological differentiation in a background of spindle cell proliferation, including myofibroblasts with various inflam-

matory components such as plasma cells, lymphocytes, and eosinophils. However, over the last three decades, inflammatory myofibroblastic tumors (IMTs) have been regarded as unique tumors with distinct clinical, pathological, and molecular features, associated with a broad spectrum of inflammatory pseudotumors (7-9).

Coffin et al. reported 84 cases of extrapulmonary IMTs in 1995 (10). Apart from somewhat lower recurrence rate (25%) and absence of metastasis, these extrapulmonary IMTs have similar clinical and histological characteristics to inflammatory fibrosarcoma. The World Health Organization (WHO) currently classifies these tumors as neoplasms of intermediate biological potential, characterized by frequent recurrence, but rare metastasis (10, 11). Coffin et al. described and classified three basic histological patterns of IMTs: Myxoid/vascular pattern, compact spindle cell pattern, and hypocellular fibrous pattern (10).

The myxoid/vascular pattern is characterized by loosely dispersed spindle to stellate myofibroblasts within an edematous/myxoid stroma, which contains abundant blood vessels with prominent infiltration by inflammatory cells, consisting of lymphocytes, plasma cells, and eosinophils. The compact spindle cell pattern is characterized by the dense and haphazard proliferation of spindle cells in a fascicular or storiform arrangement with variable myxoid and collagenized areas, accompanied by distinctive diffuse inflammatory infiltrates. Finally, the hypocellular fibrous pattern is composed of dense plate-like collagen, few spindle cells, and sparse inflammation, resembling a scar or desmoid-type fibromatosis (10-13).

There have been several studies on the histological and immunohistochemical predictors to explain the aggressive behavior of IMTs. The anaplastic lymphoma kinase (ALK) activity is one such predictor. Nearly half of IMTs exhibit clonal abnormalities, which overexpress ALK, suggesting a neoplastic cause. The ALK positivity was correlated with local recurrence, but not distant metastasis (14-16). Generally, IMTs can occur anywhere in the body, with the lungs being the most common site of IMT. Evidence shows that 43% of extrapulmonary IMTs arise from the mesentery and omentum. However, they may occur almost anywhere in the body, including the soft tissue, mediastinum, gastrointestinal (GI) tract, pancreas, genitourinary tract, oral cavity, skin, breast, bone, and central nervous system (17-20).

Generally, the GI tract involvement in IMT is rare. The description of GI IMT in the radiological literature is limited to case reports of ileocecal and gastric tumors in young girls, as the most common cases; they often have imaging features suggestive of malignancy, including ulceration, wall infiltration, and extragastric extension (4, 21, 22). Although they may span at any age, IMTs have a predilection for children and adolescents. We encountered larger series of adult for its known incidence with GI IMTs. However, accurate data pertaining to the imaging findings, clinicopathological features, and aggressiveness of GI IMTs, are difficult to obtain due to the interchangeable use of the terms "inflammatory pseudotumor" and "IMT" in the few cited reports (21). Also, it remains unknown how to classify the imaging findings of GI IMT correlated with the histopathological subtype and ALK expression in immunohistochemistry for diagnosis and treatment.

2. Objectives

This study aimed to describe a series of GI IMTs in adult patients and present their multidetector computed tomography (MDCT) findings, histopathological subtypes, clinical aggressiveness, and expression of ALK and other immunohistochemical markers. Moreover, the characteristics of computed tomography (CT) scans, pathological specimens, and histological subtypes of GI IMTs in adults were investigated.

3. Patients and Methods

3.1. Patients

This study was approved by the institutional review board committee. A retrospective review of medical records was conducted at four major academic institutions over 15 years. The medical, surgical, and pathological records were accessed for all patients, using the following keywords: "Inflammatory myofibroblastic tumor," "stomach," "small bowel," and "colon." The database search yielded 13 cases of pathologically proven GI IMTs in adults. Two cases were excluded, as their CT findings or pathological data, including immunohistochemistry, were not available for review; the remaining 11 patients constituted our study population. The final study sample included eight men and three women. The mean age of the participants was 47 years (range, 17 - 76 years).

Nine patients underwent surgical resection (gastric wedge resection in two patients; segmental resection of the small bowel in four patients and colon in one patient; and right hemicolectomy in two patients), and the remaining two gastric IMTs were pathologically confirmed by ultrasound-guided core needle biopsy and endoscopic biopsy, respectively. All 11 patients underwent contrast-enhanced CT as part of a preoperative evaluation.

3.2. Imaging Techniques

All CT scans were acquired with one of the two commercially available MDCT scanners (Brilliance 64, Ingenuity Core 128; Philips Medical Systems, Cleveland, Ohio, USA, n = 8; LightSpeed Pro 16; GE Healthcare, Milwaukee, WI, USA, n = 3). The following scanning parameters were applied in this study: Detector collimation, 64 × 0.625 or 16 × 1.25 mm; helical pitch, 1.172 or 0.938; rotation time, 0.75 or 0.5 sec; and 120 kVp/200 - 250 mAs or 120 kVp/200 - 400 mAs. The CT scans were acquired during the portal venous phase, with a 72-second delay after the injection of 120 mL of a nonionic contrast material (iopromide, Ultravist 370; Schering, Berlin, Germany) through a 20-gauge angiographic catheter, inserted into a forearm vein, using an automatic power injector (MEDRAD® Stellant, Indianola, USA) at a rate of 3 - 4 mL/s.

3.3. Imaging Analysis

The MDCT scans were retrospectively reviewed by two blinded abdominal radiologists (with 14 and 7 years of experience, respectively) via consensus. The involvement site of the GI tract and the approximate size of tumors, including the mean diameter, were assessed. The imaging findings of IMTs were analyzed regarding the growth pattern (endo- or exo-luminal growth), contrast enhancement pattern, presence of tumor necrosis, and other concomitant findings. The growth pattern of the primary tumor was subjectively categorized according to the morphological pattern, such as wall thickening or solitary mass formation.

The contrast enhancement patterns of the lesions were grouped as either homogeneous or heterogeneous and compared with the adjacent bowel wall. Other concomitant CT findings were also evaluated in this study, such as the presence or absence of bowel obstruction (i.e., dilation > 2.5 cm, proximal small bowel above the tumor, and fecal stasis, called the "small-bowel feces" sign), peritumoral infiltration, peritumoral lymphadenopathy, concomitant thickening of the peritumoral bowel wall, and tumor involvement of other abdominal organs. Specific tissue characteristics, such as myxoid change or hemorrhagic necrosis on images, were correlated with the histopathological findings if MRI was applicable.

3.4. Record Review

The patients' medical records were reviewed by one of the authors (S. Y. and Y. P.) to determine each patient's clinical presentations. The patients' demographic characteristics and data were obtained from the review charts and included treatment, tumor recurrence, morbidity, mortality, and possible comorbid diseases (i.e., Castleman's disease, Hodgkin's disease, peptic ulceration, Behcet's disease, and chronic infections, such as *Campylobacter jejuni* and *Helicobacter pylori* infections).

3.5. Pathological Review

The pathological data of all patients were collected by reviewing their pathology reports and systematic review of pathological specimens and slides, including immunohistochemistry. The specimens were also reviewed by a blinded GI pathologist (with 10 years of experience). The histopathology of IMTs was divided into three basic patterns: (1) A myxoid vascular pattern, resembling granulation tissue, nodular fasciitis, or other reactive processes; (2) a compact spindle cell pattern resembling fibromatosis, fibrous histiocytoma, or a smooth muscle neoplasm; and (3) a hypocellular fibrous pattern, resembling a scar or desmoid-type fibromatosis, according to the WHO classification. The findings were confirmed in an immunohistochemical study, including ALK, vimentin, smooth muscle actin (SMA), CD34, desmin, cytokeratin, CD68, S-100, and c-Kit measurements.

3.6. Statistical Analysis

Descriptive analysis of variables was performed using SPSS version 20.0 (IBM Corp. Released 2011. IBM SPSS Statistics for Windows, Version 20.0. Armonk, NY: IBM Corp.). Continuous variables with a normal distribution are described as mean ± standard deviation (SD), and data with a skewed distribution are described as median and range. For categorical variables, frequency (n), and proportion (%) are presented.

4. Results

4.1. Clinical Findings

Nine out of 11 patients presented with abdominal pain (average duration, 3 months; range, 2-6 months). Patients also presented with a palpable mass (n = 3), diarrhea (n = 1), and melena (n = 1). There were three cases of comorbid diseases, including two cases of chronic *H. pylori* infection and one case of hypothyroidism. The outcome information was sought for all patients, with the follow-up duration ranging from 108 days to 14 years (mean ± SD: 1827.2 ± 1776.6 days) (Table 1).

Nine patients underwent surgical resection alone. One of these patients, who underwent further surgery, died of recurrent disease and tumor metastasis, while the other eight patients with complete follow-up data showed no evidence of recurrence during the follow-up. Two patients with gastric IMTs underwent medical treatment, one of whom refused surgical resection. During the long-term

Table 1. The Basic Demographic Characteristics of the Patients [a]

Characteristics	Patients (n = 11)
Age (y)	47 ± 16.9, 50 (17 - 76)
Sex	
Male	8 (72.7)
Female	3 (27.3)
Location	
Stomach	3 (27.3)
Small bowel	4 (36.4)
Large bowel	4 (36.4)
Treatment	
Resection	9 (81.8)
Medical therapy	2 (18.2)
Prognosis	1827.2 ± 1776.6
Follow-up period (days)	2 (839 and 108 days after diagnosis, respectively)
Symptom	
Abdominal pain	9 (81.8)
Palpable mass	3 (27.3)
Diarrhea	1 (9.0)
Melena	1 (9.0)
Concomitant disease	2 *Helicobacter pylori* infections and 1 hypothyroidism

[a] Values are expressed as median (range), mean ± standard deviation or No. (%).

medical treatment, the tumor gradually decreased in size, but did not completely disappear, without aggravated or metastatic tumor until the last follow-up for 14 years (Figure 1). The other gastric IMTs with hepatic metastasis showed complete remission with steroid therapy in both lesions (Figure 2).

4.2. Imaging Findings

The main MDCT findings of the patients are summarized in Table 2. The tumor location was the stomach in four cases, small bowel in four cases, and colon in three cases. The mean diameter of tumors was 5.7 cm (range, 1.4 - 15 cm). On CT scans, growth patterns according to gross morphology included wall-thickening (n = 3) and solitary mass-forming (total, n = 8; endo-luminal, n = 3; exo-luminal, n = 3; and both, n = 2) patterns.

In the solitary mass-forming pattern, the endo-luminal type was seen as a polypoid or fungating intraluminal mass (Figure 2), which was small in size (< 3.5 cm) and mimicked submucosal tumors, such as gastrointestinal stromal tumors (GISTs) on endoscopy and endoscopic ultrasound (EUS). A tumor in the distal ileum presented as

small bowel intussusception and obstruction. All three exo-luminal tumors were found to be bulky (> 7.5 cm) and focally obscuring the bowel lumen due to the mass effect; however, no resulting mechanical obstruction was observed. Two tumors appeared to protrude in both endo- and exo-luminal directions. The other three tumors with a wall-thickening pattern were seen as diffuse and marked bowel wall thickening (> 1.2 cm), without a distinct mass or mechanical obstruction (Figure 1 and 3). These tumors appeared with a wall-thickening pattern, indistinguishable from the surrounding normal GI wall.

Tumor enhancement was variable in tumors with a solitary mass-forming pattern. either homogeneous contrast enhancement with high to iso-attenuation (n = 5) or peripheral enhancement with a large area of low attenuation, presenting with variable degrees of necrosis and myxoid change (n = 2). The wall-thickening pattern showed low attenuation, without evidence of intratumoral hemorrhage or necrosis in the markedly thickened wall. Perienteric infiltration and lymphadenopathy were observed in one gastric and one ileal IMT, and these two tumors had a wall-thickening pattern. Multiple enlarged regional lymph nodes were combined in the wall-thickening pattern (Figure 1).

Distant metastasis was observed in one patient, involving the liver; it was seen as a nodule with ring-like enhancement (Figure 2). Based on additional imaging findings, internal myxoid degeneration and hemorrhage were identified in one pedunculated gastric IMT on MRI, correlated with the histopathological findings (Figure 4).

4.3. Histopathological Findings

Nine patients underwent complete tumor resection. In two patients, pathological specimens were only available through gastroscopic biopsy. The spindle myofibroblasts, fibroblasts, and inflammatory cells of all IMTs showed a mixture of variable histological patterns. Seven IMTs were classified as compact spindle cell patterns, and four IMTs were classified as myxoid vascular patterns. No IMT with a hypocellular fibrous pattern was observed in the study. Due to the limitations of retrospective studies, sufficient immunohistochemical analyses could not be confirmed in all patients. Among cases with confirmed results, all patients were negative for ALK, S-100, and desmin and positive for vimentin (Table 3).

Three myxoid vascular pattern masses represented a wall-thickening pattern in the stomach, ileum, and colon. One myxoid vascular pattern showed a discrete solitary mass-forming pattern in the ileum. Seven masses with a compact spindle cell pattern represented a solitary mass-forming pattern in the stomach (n = 3), small bowel (n = 2), and colon (n = 2). One gastric IMT with hepatic metastasis
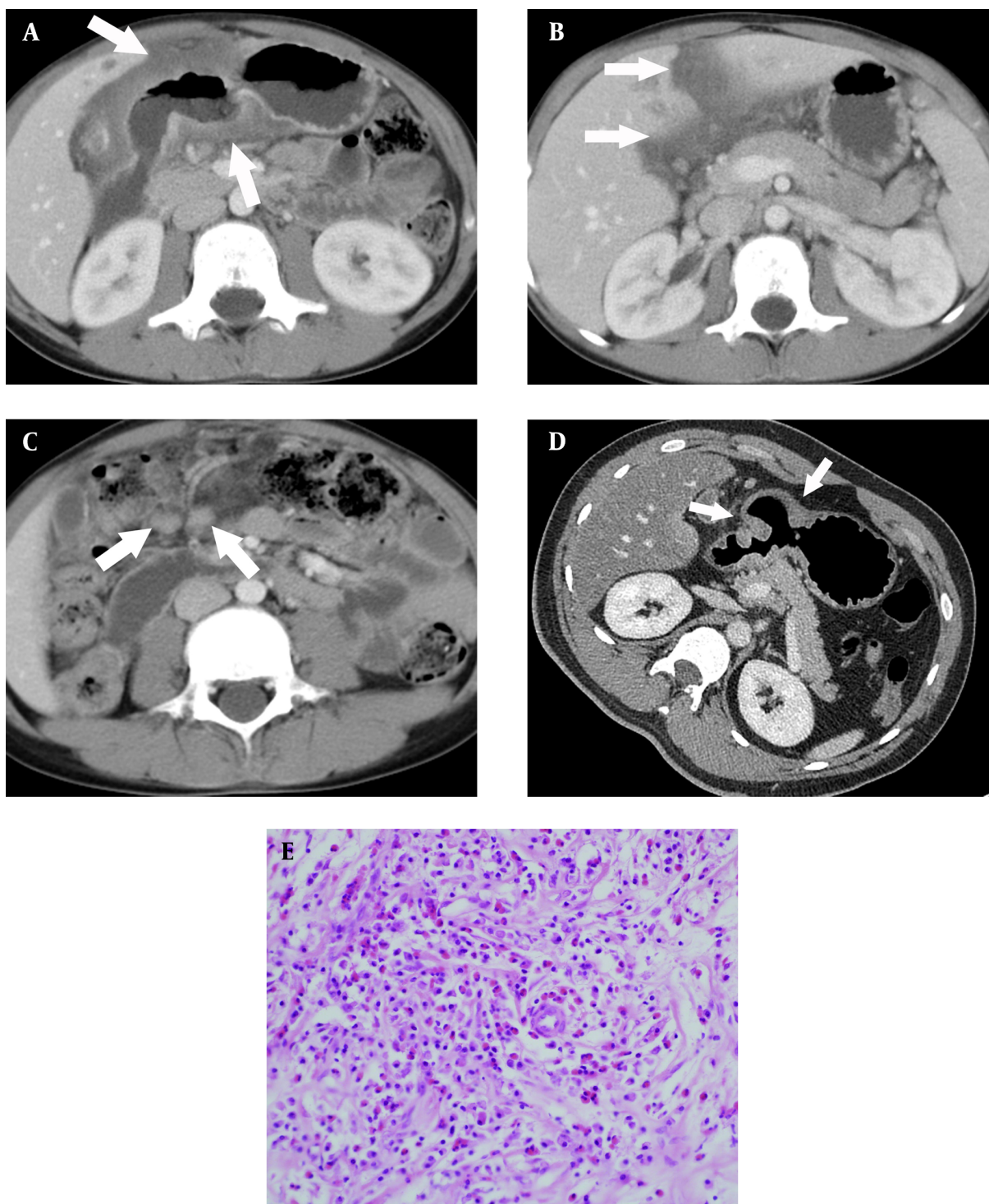
Figure 1. A 17-year-old man with an inflammatory myofibroblastic tumor in the gastric antrum. A, Contrast-enhanced computed tomography (CT) scan showing low-attenuating wall thickening (arrows) in the gastric antrum with severe perigastric infiltration. There is mucosal disruption, indicating the presence of a large mucosal ulcer; B, Perigastric infiltration (arrows) extends to the hepatoduodenal ligament and falciform ligament; C, Multiple enlarged lymph nodes (arrows) are seen along the greater curvature side of the gastric antrum; D, Contrast-enhanced CT taken 14 years after medical treatment shows remnant wall thickening in the gastric antrum with a bulging appearance (arrows), besides the improved state of perigastric infiltration; and E, The photomicrograph (Hematoxylin and Eosin [H&E] staining, 400X staining) shows loosely arranged spindle-shaped tumor cells with abundant blood vessels and an infiltrate of inflammatory cells, including plasma cells and eosinophils.
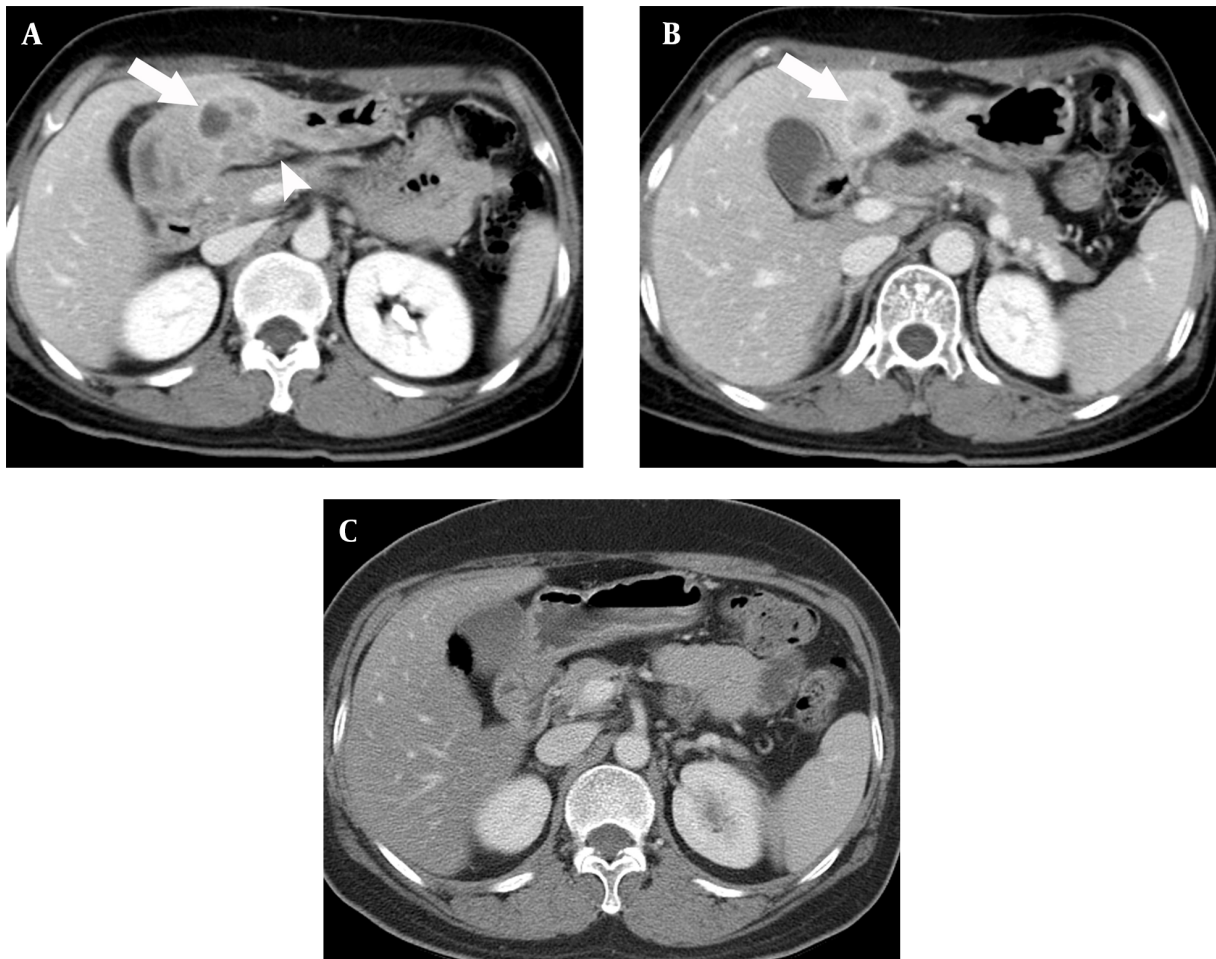
Figure 2. A 49-year-old woman with an inflammatory myofibroblastic tumor in the gastric antrum. A, Contrast-enhanced computed tomography (CT) scan showing a heterogeneous enhancing mass (arrow) in the thickened wall of the gastric antrum. Perigastric infiltration (arrowhead) extends to the gastrohepatic ligament; B, A targetoid enhancing mass lesion (arrow) is seen in the liver. Perigastic infiltration extends to the gastrohepatic ligament; and C, Contrast-enhanced CT scan taken 11 months after medical treatment shows complete remission of both tumor lesions.

showed complete remission with steroid therapy in both lesions (Figure 2). The solitary mass-forming pattern in the stomach was pathologically confirmed as a compact spindle cell pattern. The tumor showed negative results for S-100, c-Kit, CD34, ALK, cytokeratin, and desmin and positive results for SMA and vimentin. The only mass that was positive for CD34 showed a solitary mass-forming pattern in the ileum and a myxoid vascular pattern, which was seen as a loosely arranged feature on microscopic imaging.

5. Discussion

The MDCT images of 11 IMTs, which primarily developed in the GI tract, were reviewed in this study. The MDCT findings of GI IMTs can be classified into two patterns: Wall-thickening and solitary mass-forming patterns.

Each growth pattern was well matched with a characteristic pathological pattern: Wall-thickening pattern with the myxoid-vascular pattern and solitary mass-forming pattern with compact spindle cell pattern. In the present study, the GI IMTs met the requirements of only two of the three main pathological patterns, that is, compact spindle cell pattern and myxoid vascular pattern.

Tumors with the myxoid vascular pattern showed similar findings to those of GI tract lymphoma, which could present as infiltrative wall thickening or a well-circumscribed mass unassociated with intestinal obstruction, even if the mass is large. Tumors with a compact spindle cell pattern showed similar findings to those of subepithelial tumors, such as GIST, but they did not exhibit hypervascularity. There was no bowel obstruction in either

Table 2. The Computed Tomography Imaging Findings of Inflammatory Myofibroblastic Tumors [a]

Characteristics	Myxoid vascular pattern (n = 4)	Compact spindle cell pattern (n = 7)
Age (y)	42 (17 - 52)	52 (19 - 76)
Sex (M: F)	3:1	5:2
Size (mm)	58.3 ± 34.53	41.1 ± 26.2
Gross morphology		7 (100)
Mass forming	1 (25)	
Wall thickening	3 (75)	
Tumor location		
Stomach	1 (25)	3 (42.9)
Small bowel	2 (50)	2 (28.6)
Large bowel	1 (25)	2 (28.6)
Distant metastasis		1 (14.3)
Lymph node enlargement	2 (50)	1 (14.3)
Homogeneous enhancement	3 (75)	5 (71.4)
Heterogeneous enhancement with intratumoral low attenuation	1 (25)	2 (28.6)
Intussusception	1 (25)	1 (14.3)

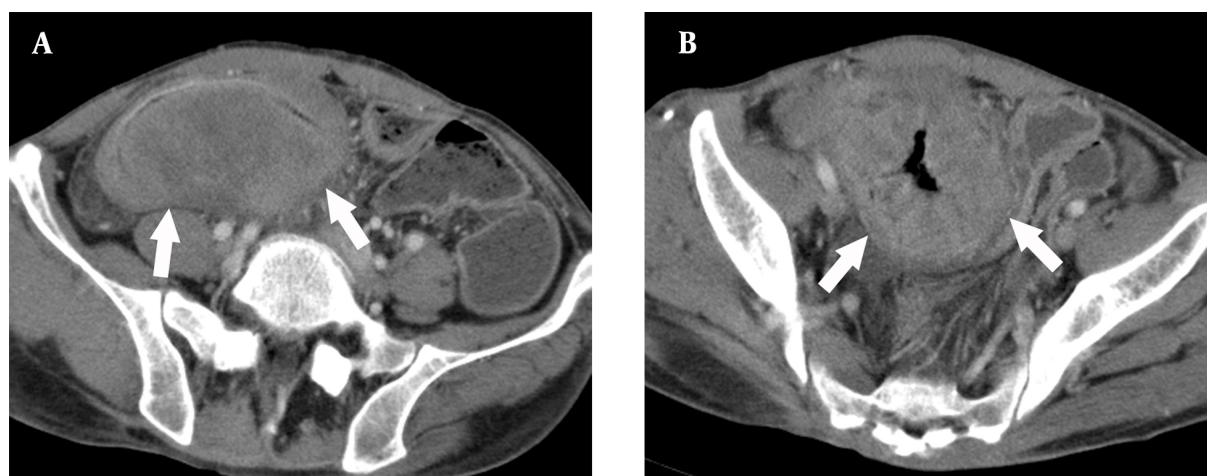[a] Values are expressed as median (range), mean ± standard deviation or No. (%).

Figure 3. A 52-year-old man with a loosely arranged inflammatory myofibroblastic tumor in the ileum. A, Contrast-enhanced computed tomography (CT) scan showing a low-density mass with unclear margins (arrows) and low-density wall thickening around it; B, There is very severe wall thickening (arrows), as well as peripheral infiltration, but no bowel obstruction.

type of GI IMT despite its large size, except two cases, which showed intraluminal growth and small bowel intussusception.

Since GI IMT is generally a rare disease, imaging findings are not well-established, and their relationship with disease prognosis has not been sufficiently studied. In this regard, Lee et al. examined five IMTs of the stomach and reported that gastric IMT appeared with two features, including a well-defined subepithelial tumor or irregular wall thickening, with a commonly strong enhancement (23). This appearance is consistent with the results of the present study on the IMT of the entire GI tract. It has been reported that larger lesions may result in central necrosis (4). There was no significant difference between the two pathological patterns of IMTs. In a study investigating abdominal IMT imaging findings, including the bowel, liver, and mesentery, it was reported that the compact cell type and hypocellular fibrous type formed a mass with discrete
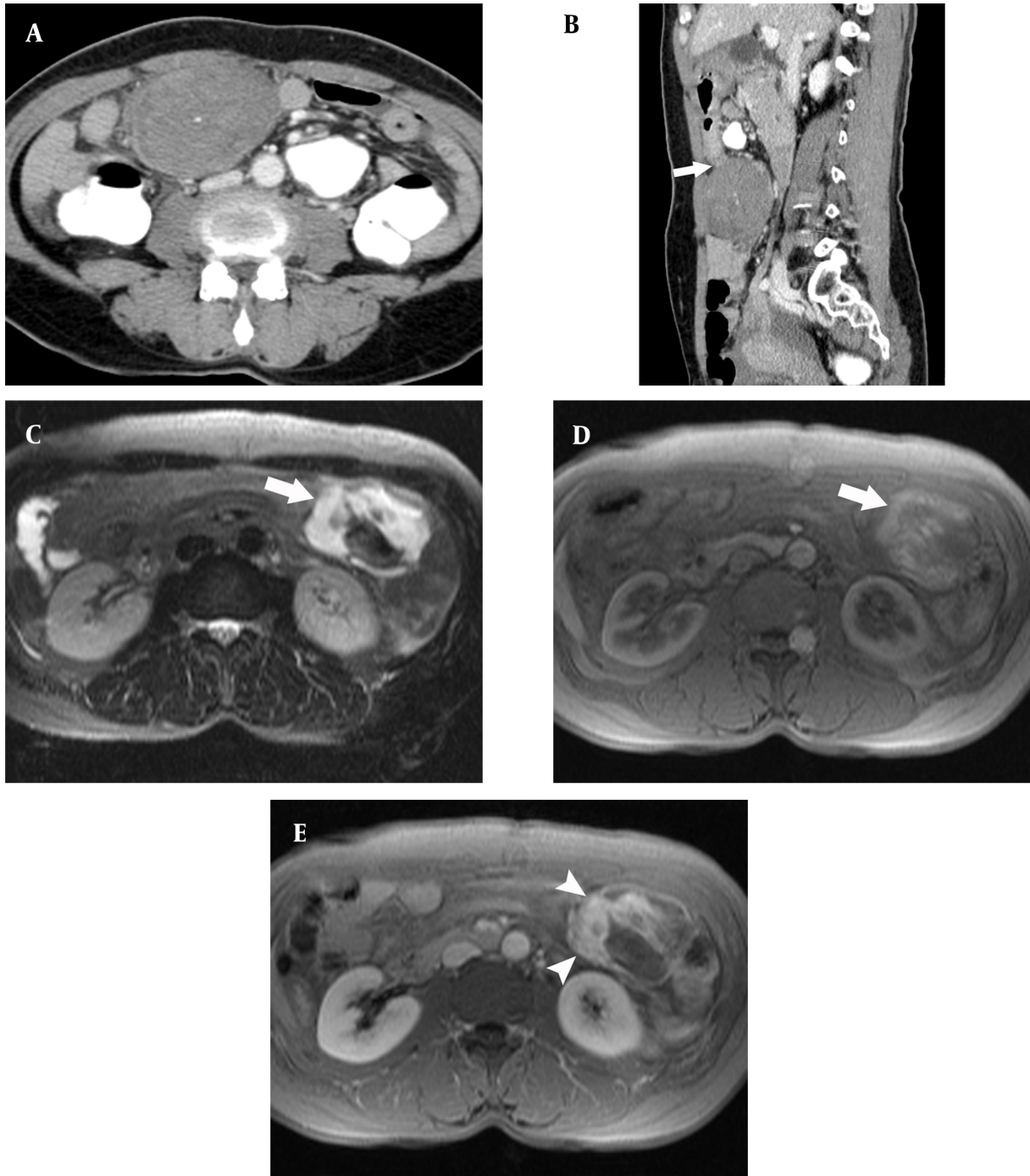
Figure 4. A 55-year-old woman with a compactly arranged inflammatory myofibroblastic tumor in the gastric antrum. A, A well-defined low-density mass is seen in the greater curvature side of the gastric antrum; B, The mass shows an exophytic pedunculated appearance (arrow) at the gastric antrum; C, Fat-saturated T2-weighted MR image shows T2 signal hyperintensity (arrow) in the mass; D, Pre-contrast T1-weighted image shows high signal intensity (arrow) in the mass, representing hemorrhage; and E, Contrast-enhanced T1-weighted image shows that the part of the mass with high signal intensity in the T1-weighted image becomes contrast-enhanced (arrowheads), representing the myxoid component.

Table 3. The Immunohistochemical Results of Inflammatory Myofibroblastic Tumors [a]

Immunohistochemical results	Myxoid vascular pattern (n = 4)	Compact spindle cell pattern (n = 7)
Immunohistochemical stain		
Vimentin	4 (100)	7 (100)
ALK	0	0
Desmin	0	0
SMA	4 (100)	5 (71.4)
S-100	0	0
CD68	3 (75)	2 (28.6)
CD34	1 (25)	0

Abbreviations: SMA, smooth muscle actin; ALK, anaplastic lymphoma kinase.
[a] Values are expressed as No. (%).

margins, which is also consistent with our findings (11).

Inflammatory myofibroblastic tumor has emerged as a distinct disease entity with characteristic clinical, pathological, and molecular features, although the term "inflammatory pseudotumor" has been used to describe a wide range of reactive and neoplastic lesions (2). It is known that chromosomal translocations leading to the activation of ALK tyrosine kinase can be detected in approximately half of IMTs; these features are known to suggest neoplasms of clonal change rather than reactive changes caused by inflammation (2). Coffin et al. reported that ALK-negative IMTs were associated with older age and a higher rate of distant metastasis (15). In the current study, there were no ALK-positive IMT patients. This result is because of the fact that patients in this study were relatively older than those with the usual features of IMT; these findings are consistent with the results of the previous study by Coffin et al. (15).

Additionally, it is known that a large part of inflammatory pseudotumor involves immunoglubulin G4 (IgG4) infiltration in the serum and tissues, which is classified as an inflammatory pseudotumor associated with IgG4-related sclerosing disease (24). Immunoglubulin G4-related inflammatory pseudotumors show typical microscopic features, including infiltration of many lymphocytes, IgG4-positive plasma cells, fibrosclerosis, and obstructive phlebitis. Compared to IMT, IgG4-related inflammatory pseudotumor usually develops in older patients and is commonly associated with autoimmune pancreatitis and sclerosing cholangitis. However, in the present study, IgG4 immunofluorescence stain for histological specimens and IgG4 serum level test were not performed for all cases. In this study, findings, such as diffuse infiltration of inflammatory cells with prominent plasma cells

and low mitotic rate without atypical forms, were consistent with features suggestive of IMT.

The IMTs are known to be tumors of intermediate malignancy potential according to the WHO classification due to their tendency for local recurrence and a low risk of distant metastasis (2). The recurrence of IMT following resection has been reported in 18% to 40% of cases and appears to be higher in extrapulmonary lesions, which are larger than 8 cm or locally invasive (22). In our patients, hepatic metastasis was found in gastric IMT with a compact spindle cell pattern. There was no tumor recurrence in IMTs with a compact spindle cell pattern during the follow-up. Two patients with IMTs of myxoid vascular pattern showed perienteric infiltration and regional lymphadenopathy, one of whom experienced local recurrence after surgery.

The usual treatment for IMT is surgical resection, and additional chemotherapy is required if the surrounding invasion is severe, or if there is metastasis. However, some studies have reported improvements by administering anti-inflammatory drugs, including steroids and non-steroidal anti-inflammatory drugs (25, 26). However, it is not known which medical therapy is effective for which pathological type. It is assumed that medical treatment using anti-inflammatory drugs can be more helpful for the treatment of tumors containing various inflammatory cells, with severe infiltration into the surrounding area. However, further study on a larger sample size is needed. In the present study, steroid treatment caused improvements without any need for surgery; the tumor was a compact cell type with a solitary mass-forming pattern.

This study has several limitations. First, the sample size was limited. Only 11 patients were included in this study because of the rarity of GI IMTs. Therefore, all cases showed negative results for ALK, and no hypocellular fibrous pattern was included. Also, the clinical significance of each immunohistochemical study could not be evaluated; therefore, further research should be conducted on a sufficient sample size. Second, the follow-up period was relatively short. The duration of follow-up ranged from seven months to seven years (mean, 5 years); consequently, we cannot rule out the possibility of late-onset metastasis after treatment. Third, there may be conflicts regarding the pathological type of IMT. In some cases, it was difficult to determine the histological subtype, because there were overlapping areas of two histological subtypes; the main histological subtype was determined according to its composition. Finally, the CT protocol was inconsistent, because multicenter cases over a long period were collected, and quantitative analyses, such as texture analysis or dynamic enhancement pattern, could not be performed.

In conclusion, the imaging findings of GI IMTs in adults on CT scans can be classified into two patterns:

Wall-thickening and solitary mass-forming patterns. Each growth pattern was well-matched with a characteristic pathological subtype (myxoid vascular pattern or compact spindle cell pattern), which could help explain the tumor behavior. Based on the findings, GI IMTs might show different biological potentials according to the histopathological subtype.

Footnotes

Authors' Contributions: Study concept and design: S. Y. and B. P.; acquisition of data: S. Y., D. S., M. K., Y. P., and S. K.; analysis and interpretation of data: S. C. and J. C.; drafting of the manuscript: I. C. and N. H.; critical revision of the manuscript for important intellectual content: S. Y.; statistical analysis: B. P.; administrative, technical, and material support: S. Y.; and study supervision: S. Y.

Conflict of Interests: This study was supported by a grant from Korea University Research Grant (grant No.: K1925111 by Dr. Choi.). The authors have no affiliations to institutions other than their hospitals and are not employed by any other company. The authors have no financial interests related to this study. They are not affiliated to any governmental agencies and are not editorial board members or reviewers of this journal.

Data Reproducibility: The dataset presented in this study is available on request from the corresponding author during submission or after its publication. The data are not publicly available due to the inclusion of the clinical images of the patients.

Ethical Approval: This study was approved under the institutional review board approval code, 2018AS0292 (link: irb.kumc.or.kr/Study/ResearchTab.aspx).

Funding/Support: This research was supported by the Korea University Research Grant (grant No.: K1925111 by Dr. Choi.).

References

1. Umiker WO, Iverson L. Postinflammatory tumors of the lung; report of four cases simulating xanthoma, fibroma, or plasma cell tumor. *J Thorac Surg*. 1954;**28**(1):55–63. [PubMed ID: 13175281].
2. Gleason BC, Hornick JL. Inflammatory myofibroblastic tumours: where are we now? *J Clin Pathol*. 2008;**61**(4):428–37. [PubMed ID: 17938159]. https://doi.org/10.1136/jcp.2007.049387.
3. Siemion K, Reszec-Gielazyn J, Kisluk J, Roszkowiak L, Zak J, Korzynska A. What do we know about inflammatory myofibroblastic tumors? - A systematic review. *Adv Med Sci*. 2022;**67**(1):129–38. [PubMed ID: 35219201]. https://doi.org/10.1016/j.advms.2022.02.002.
4. Narla LD, Newman B, Spottswood SS, Narla S, Kolli R. Inflammatory pseudotumor. *Radiographics*. 2003;**23**(3):719–29. [PubMed ID: 12740472]. https://doi.org/10.1148/rg.233025073.
5. Park SB, Cho KS, Kim JK, Lee JH, Jeong AK, Kwon WJ, et al. Inflammatory pseudotumor (myoblastic tumor) of the genitourinary tract. *AJR Am J Roentgenol*. 2008;**191**(4):1255–62. [PubMed ID: 18806173]. https://doi.org/10.2214/AJR.07.3663.
6. Patnana M, Sevrukov AB, Elsayes KM, Viswanathan C, Lubner M, Menias CO. Inflammatory pseudotumor: the great mimicker. *AJR Am J Roentgenol*. 2012;**198**(3):W217–27. [PubMed ID: 22358018]. https://doi.org/10.2214/AJR.11.7288.
7. Meis JM, Enzinger FM. Inflammatory fibrosarcoma of the mesentery and retroperitoneum. A tumor closely simulating inflammatory pseudotumor. *Am J Surg Pathol*. 1991;**15**(12):1146–56. [PubMed ID: 1746682]. https://doi.org/10.1097/00000478-199112000-00005.
8. Cook JR, Dehner LP, Collins MH, Ma Z, Morris SW, Coffin CM, et al. Anaplastic lymphoma kinase (ALK) expression in the inflammatory myofibroblastic tumor: a comparative immunohistochemical study. *Am J Surg Pathol*. 2001;**25**(11):1364–71. [PubMed ID: 11684952]. https://doi.org/10.1097/00000478-200111000-00003.
9. Carrasco Rodriguez R, Garcia Fontan EM, Blanco Ramos M, Magdalena Benavides LJ, Otero Lozano D, Moldes Rodriguez M, et al. Inflammatory pseudotumor and myofibroblastic inflammatory tumor. Diagnostic criteria and prognostic differences. *Cir Esp (Engl Ed)*. 2022;**100**(6):329–35. [PubMed ID: 35577280]. https://doi.org/10.1016/j.cireng.2022.05.012.
10. Coffin CM, Watterson J, Priest JR, Dehner LP. Extrapulmonary inflammatory myofibroblastic tumor (inflammatory pseudotumor). A clinicopathologic and immunohistochemical study of 84 cases. *Am J Surg Pathol*. 1995;**19**(8):859–72. [PubMed ID: 7611533]. https://doi.org/10.1097/00000478-199508000-00001.
11. Coffin CM, Humphrey PA, Dehner LP. Extrapulmonary inflammatory myofibroblastic tumor: a clinical and pathological survey. *Semin Diagn Pathol*. 1998;**15**(2):85–101. [PubMed ID: 9606801].
12. Kapusta LR, Weiss MA, Ramsay J, Lopez-Beltran A, Srigley JR. Inflammatory myofibroblastic tumors of the kidney: a clinicopathologic and immunohistochemical study of 12 cases. *Am J Surg Pathol*. 2003;**27**(5):658–66. [PubMed ID: 12717250]. https://doi.org/10.1097/00000478-200305000-00009.
13. Gasparotti R, Zanetti D, Bolzoni A, Gamba P, Morassi ML, Ungari M. Inflammatory myofibroblastic tumor of the temporal bone. *AJNR Am J Neuroradiol*. 2003;**24**(10):2092–6. [PubMed ID: 14625240]. [PubMed Central ID: PMC8148917].
14. Hussong JW, Brown M, Perkins SL, Dehner LP, Coffin CM. Comparison of DNA ploidy, histologic, and immunohistochemical findings with clinical outcome in inflammatory myofibroblastic tumors. *Mod Pathol*. 1999;**12**(3):279–86. [PubMed ID: 10102613].
15. Coffin CM, Hornick JL, Fletcher CD. Inflammatory myofibroblastic tumor: comparison of clinicopathologic, histologic, and immunohistochemical features including ALK expression in atypical and aggressive cases. *Am J Surg Pathol*. 2007;**31**(4):509–20. [PubMed ID: 17414097]. https://doi.org/10.1097/01.pas.0000213393.57322.c7.
16. Logaswari M, Lim KHT, Tan D, Ong CJ, Sittampalam K. Inflammatory myofibroblastic tumour of the rectum with a novel anaplastic lymphoma kinase fusion diagnosed on cytology: Not just another submucosal gastrointestinal stromal tumour!. *Cytopathology*. 2022;**33**(3):397–401. [PubMed ID: 35118731]. https://doi.org/10.1111/cyt.13108.
17. Ramachandra S, Hollowood K, Bisceglia M, Fletcher CD. Inflammatory pseudotumour of soft tissues: a clinicopathological and immunohistochemical analysis of 18 cases. *Histopathology*. 1995;**27**(4):313–23. [PubMed ID: 8847061]. https://doi.org/10.1111/j.1365-2559.1995.tb01521.x.
18. Hausler M, Schaade L, Ramaekers VT, Doenges M, Heimann G, Sellhaus B. Inflammatory pseudotumors of the central nervous system: report of 3 cases and a literature review. *Hum Pathol*. 2003;**34**(3):253–62. [PubMed ID: 12673560]. https://doi.org/10.1053/hupa.2003.35.
19. Markovic Vasiljkovic B, Plesinac Karapandzic V, Pejcic T, Djuric Stefanovic A, Milosevic Z, Plesinac S. Follow-Up Imaging of Inflammatory Myofibroblastic Tumor of the Uterus and Its Spontaneous Regression.

Iran J Radiol. 2016;**13**(1). e12991. [PubMed ID: 27110328]. [PubMed Central ID: PMC4835684]. https://doi.org/10.5812/iranjradiol.12991.

20. Rich BS, Fishbein J, Lautz T, Rubalcava NS, Kartal T, Newman E, et al. Inflammatory myofibroblastic tumor: A multi-institutional study from the Pediatric Surgical Oncology Research Collaborative. *Int J Cancer.* 2022;**151**(7):1059–67. [PubMed ID: 35604778]. https://doi.org/10.1002/ijc.34132.

21. Janik JS, Janik JP, Lovell MA, Hendrickson RJ, Bensard DD, Greffe BS. Recurrent inflammatory pseudotumors in children. *J Pediatr Surg.* 2003;**38**(10):1491–5. [PubMed ID: 14577073]. https://doi.org/10.1016/s0022-3468(03)00501-3.

22. Sanders BM, West KW, Gingalewski C, Engum S, Davis M, Grosfeld JL. Inflammatory pseudotumor of the alimentary tract: clinical and surgical experience. *J Pediatr Surg.* 2001;**36**(1):169–73. [PubMed ID: 11150459]. https://doi.org/10.1053/jpsu.2001.20045.

23. Lee JE, Choi SY, Lee HK, Yi BH, Lee MH, Lee S, et al. Computed tomographic features of inflammatory myofibroblastic tumour of the stomach in adult patients: An analysis of five multicentre cases with literature review. *J Med Imaging Radiat Oncol.* 2018;**62**(6):769–76. [PubMed ID: 30076671]. https://doi.org/10.1111/1754-9485.12780.

24. Yamamoto H, Yamaguchi H, Aishima S, Oda Y, Kohashi K, Oshiro Y, et al. Inflammatory myofibroblastic tumor versus IgG4-related sclerosing disease and inflammatory pseudotumor: a comparative clinicopathologic study. *Am J Surg Pathol.* 2009;**33**(9):1330–40. [PubMed ID: 19718789]. https://doi.org/10.1097/pas.0b013e3181a5a207.

25. Fragoso AC, Eloy C, Estevao-Costa J, Campos M, Farinha N, Lopes JM. Abdominal inflammatory myofibroblastic tumor a clinicopathologic study with reappraisal of biologic behavior. *J Pediatr Surg.* 2011;**46**(11):2076–82. [PubMed ID: 22075336]. https://doi.org/10.1016/j.jpedsurg.2011.07.009.

26. Su W, Ko A, O'Connell T, Applebaum H. Treatment of pseudotumors with nonsteroidal antiinflammatory drugs. *J Pediatr Surg.* 2000;**35**(11):1635–7. [PubMed ID: 11083441]. https://doi.org/10.1053/jpsu.2000.18340.